



# Computer Modeling Application for Analysis of Stress-Strain State of Vibroscreen Feed Elements by Finite Elements Method

M. Doudkin<sup>1</sup>(✉), A. Kim<sup>1</sup>, V. Kim<sup>1</sup>, M. Mlynczak<sup>2</sup>, and G. Kustarev<sup>3</sup>

<sup>1</sup> D. Serikbayev East Kazakhstan State Technical University,  
19, Serikbayev Str., Ust-Kamenogorsk, Kazakhstan  
vas\_dud@mail.ru, k.a.i.90@mail.ru, k-v-a@list.ru

<sup>2</sup> Wroclaw University of Science and Technology,  
27, Wybrzeze Wyspianskiego, 50-370 Wroclaw, Poland  
marek.mlynczak@pwr.edu.pl

<sup>3</sup> Moscow Automobile and Road Construction State Technical University,  
64, Leningradsky Prospect, Moscow, Russian Federation  
proektdm@mail.ru

**Abstract.** The article presents a three-dimensional solid-state computational model, as well as the results of stress-strain state analysis of feed elements rods of vibroscreen. An algorithm for solving the problem numerically using the finite element method is proposed. The obtained results were used at the designing stage of the platform with feed elements for industrial vibroscreen and subsequently confirmed in work in a real experiment. The stress-strain state of feed elements rods was analyzed for various bulk materials, conditionally designated A and B, sorted by vibrating screen, where feed elements were mounted. These materials, in screening process with varying strength, acted on feed elements rods, the parameters of which did not change for the flow of various bulk materials. Rods perceived this load pressing in different ways, which was shown by the finite element analysis.

**Keywords:** Vibroscreen · Feed elements · Analysis ·  
Finite elements method · Modeling

## 1 Introduction

The proposed article is in addition to the well-known publication “New vibroscreen with additional feed elements” [1], which describes the mathematical and physical models of the experimental installation of a new vibroscreen with additional feed elements. Feed elements are an additional construction that significantly intensifies the screening process and at the same time the weakest part of the vibroscreen. Based on the developed mathematical screening model using a

main platform of feed elements, numerical studies have been carried out to identify the influence of the process parameters on the screening kinetics and the state of various passage particles in the screened layer. The numerical studies shown that the introduction of additional feed elements into the screened material flow leads to an increase in the passing intensity of the bulk material lower class to the sieve, regardless of the size fractions of different bulk materials.

Figure 1 schematically shows a vibrator with additional feed elements (FE) 7 mounted on the frame 6.

During the screening process, the sorted material flow 2 moves along the screen 1 and comes into contact with the feed elements (FE) 7 located along and across the screen. Since the feed elements themselves are installed with a certain step, the material not only rests against them, but also flows around the sides, exerting pressure on them with a certain force for each material.

The collision of bulk material particles with FE leads to the creation of additional chaotic movements of particles in the upper layers of bulk material, either coinciding or different from the forced oscillations direction from the vibration exciter 5 (Fig. 1). While the difference in particles velocities of the particulate material relative to each other, which activates the passing particles process of the bottom fraction to the screen surface through the entire layer of bulk material through forced mixing.

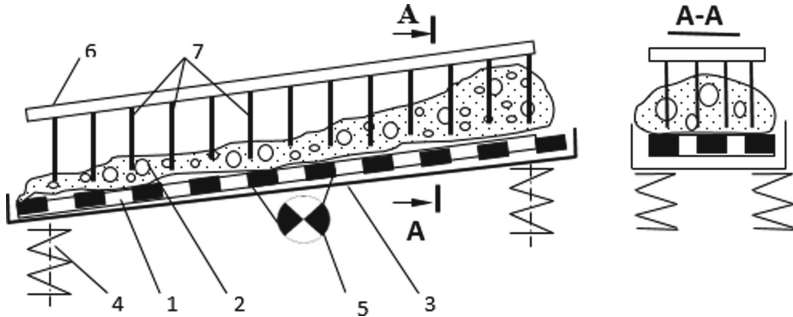


**Fig. 1.** Scheme of vibroscreen with additional feed elements: 1 - screen, 2 - bulk material, 3 - box, 4 - elastic supports, 5 - vibration engine, 6 - frame, 7 - feed elements.

The productivity of screening before FE can be described by the formula [1]:

$$Q = \mu_{FE} \cdot (S - S_{FE}) \cdot \sqrt{\frac{2}{\gamma - \Delta\gamma} \left( \frac{m(t) \cdot (0.02 \cdot A \cdot \vartheta^2)}{S} - \frac{k_F \cdot \gamma(t) \cdot c \cdot (2.22 \cdot A \cdot \vartheta^2)}{2} \right)} \quad (1)$$

It can be seen from the formula (1) that the increase in the productivity of the screening process is possible due to decrease in the specific material mass on the screen or by more intensive mixing of the bulk material on the screen, which

leads to slowing down of the material flow, as well as its redistribution and longer residence of the material in the active sieving zone. As a result, the specific weight of the finished product increases, the total amount of material decreases, while the productivity  $Q$  increases; because smaller amount of material is distributed over the same area of material flow and experiences less resistance.

Since active screening occurs mainly up to FE, after them the vibrating screen can be considered as a vibration transporter, since the screening process after FE itself is very insignificant, so that the productivity of the process after FE is directly and primarily related to the speed of material transportation along the screen  $Q = v(t)$ , and velocity of the material passing through the screen is the main researched parameter after the FE [1–6].

$$\frac{\nu_2^2}{\nu^2} = \frac{2m \cdot A_2 \cdot \vartheta^2 \cdot \phi_2^2}{S_2 \cdot (\gamma - \Delta\gamma)} \cdot \frac{S \cdot \gamma(t)}{2m \cdot A \cdot \vartheta^2 \cdot \phi^2} \Rightarrow \frac{\nu_2^2}{\nu^2} = \frac{A_2 \cdot \phi_2^2 \cdot \gamma \cdot S}{A \cdot \phi^2 \cdot (\gamma - \gamma_2) \cdot S_2}. \quad (2)$$

According to the formula (2), it can be concluded that the rate of bulk material after FE should increase for the following reasons:

- due to the decrease in the material resistance to movement, because, after the FE, the number of material pieces decreases per area, respectively, the pieces of the remaining material less interfere with each other;
- in connection with the increase in energy, i.e. at each point, a certain energy was initially supplied, which depended on the amplitude and frequency of sieve vibrations, and after the FE, with a decrease in the specific material mass, which was partially sorted and fell into the subsystem space, the energy that was set for the entire volume of the bulk material was now consumed only on his remaining part.

After substituting the experimental data into the formula (2), mathematical calculations confirmed the tendency of first screening phase acceleration, i.e. the time of material passage to the screen is accelerated by the use of additional FEs at 6.66% with the use of static FE and by 13.33%, with the use of dynamic FE, the overall efficiency of the screening process is accordingly increased, which is graphically depicted in Fig. 2, each state of a vibrating screen (a - without a FE; b - with static RE; c - with dynamic FE) as an increase in the upper horizontal coordinate shows the acceleration of the first screening phase for 6 cells, conventionally accepted lying on the screen.

To carry out experimental studies and analyze the behavior of particles on a natural flat screen, a physical model of vibrating screen was developed and manufactured, which contains a sieve box mounted on elastic supports, vibrator and installed feed elements (FE) above the surface of the screen, rods attached to the frame, while the feed elements can be movable and equipped with a drive, and also fixed removable [7–12].

These requirements, even before the production of feed elements complex, lead to the need for setting new tasks and developing new modeling techniques at the stage of feed elements designing for vibration screens that most fully and

adequately take into account the geometry, internal composition and mechanical features of the elements being developed for operation under real operating conditions.

From these conditions, higher requirements to the rigidity and strength of the feed elements arise, while simultaneously striving to reduce their mass, optimality and versatility of the design, while maintaining the reliability of the work and the FE, and the vibroscreen itself.

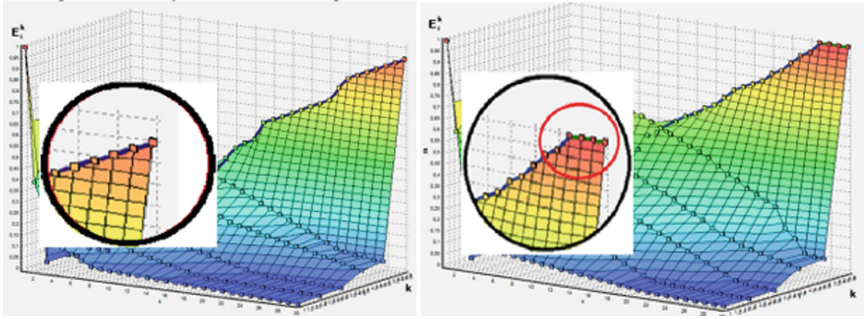


**Fig. 2.** Graphic image of the acceleration of the first screening phase of the conditional 6th cell: (a) conventional vibroscreen (without FEs); (b) vibroscreen with static FEs; (c) vibroscreen with dynamic FEs, according to the developed mathematical model.

## 2 FEM Analysis

One of the main methods that reduce the structure development time, which increasing requirements for rigidity and strength characteristics, is the finite element method (FEM), which makes it possible to foresee the behavior and reliability of the experimental design, even before industrial manufacture. This makes it possible to shorten the cycles of experimental studies, modification of the design, processing of design and technological documentation, significant reduction in the cost of production preparation.

Therefore, the analysis of design decisions in the early design stages with the help of simulation systems, including the finite element analysis, which allows modeling the future design and the processes of its testing for various effects at the design stage, acquires special significance.

In this article, the finite element method (FEM) is used to solve the problems of determining the stress-strain state of feed elements rods fixed on the platform, for which we will perform the necessary preliminary graphic constructions, calculations and selection of initial data.

A solid 3D model of a vibrating screen with a separate bearing surface of feed elements rods (Fig. 3) and separate calculation models (Figs. 4, 5, 6 and 7) of feed elements consisting of metal rods mounted on a bearing platform from metal

corners were developed and implemented in a system of parametric solid modeling KOMPAS-3DV17.1. The calculations were made in the APM FEM system, which is an integrated tool in the KOMPAS-3DV17.1 for the preparation and subsequent finite element analysis of a three-dimensional solid model (Certification passport No. 330 dated April 18, 2013, issued by the Federal Service for Environmental, Technological and Nuclear Supervision (Rostekhnadzor), FBU “STC NRS”). The calculating core of the APM FEM system for KOMPAS-3D is the “Finite element program system APM Structure 3D [13–17].

In the considered structure of the vibroscreen, the investigated element will be a system of feed elements consisting of a bearing surface and eight vertical rods arranged 4 in two rows and at a certain distance from each other (Fig. 3).

The setting of the feed elements on the vibrating screen is shown in Fig. 3. The calculated finite element grid of the platform with feed elements is shown in Fig. 4. Between feed elements by conditional groups, the sorted material with a shadow trace from the motion is shown schematically.

Conditionally it is considered that the bulk material flow during the passage of the feed elements rods is the same in height both in the middle of the screen and at edges, which is shown in Figs. 5, 6 and 7.

The structure of the feed elements can be conditionally divided into two groups of homogeneous elements - a metal corner (Steel 20, Table 1), from which the bearing platform is made (Corner profile d63x63x5 GOST 8509-93, transverse length  $L = 1066$  mm and longitudinal length  $L = 340$  mm), which serves as the basis for fastening the rods, and the rods themselves (Steel 45, GOST 1050-2013), mounted on this site.

The behavior of feed elements is simulated in contact with two different bulk materials “A” and “B”, which have significant property differences. For each distributed force acting on feed elements, the corresponding objects are selected and the following load parameters are applied: Force vector: for material “A” -  $X = 400$ ;  $Y = 0$ ;  $z = 0$ ; for material “B” -  $X = 1200$ ;  $Y = 0$ ;  $z = 0$ . Accordingly, the magnitude of the flow force of the bulk material acting on the rods of the feed elements: for material “A” - 400 N, for material “B” - 1200 N.

Accordingly, information on fixations and coinciding surfaces is included in the program, and finite-element grid consisting of 10 nodal tetrahedrons is chosen. It should be noted that tetrahedrons are the only elements that can be used to thicken the adaptive grid. When the density of the grid is increased, the solution becomes more precise. So it can unerringly assume relatively slow change in the stresses in these areas. In these calculations, the adaptive grid is unchanged. For all accepted parameters, static calculations were performed, the results of which are presented in Figs. 4, 5, 6 and 7.

The initial data for solving the problem are summarized in Tables 1, 2 and 3.

The equivalent Mises stress (Fig. 5), SVM (MPa), ranged from the minimum value (0) to the maximum (118,579,194) for bulk material “A” and from 0 to 474.317501 for material “B”.

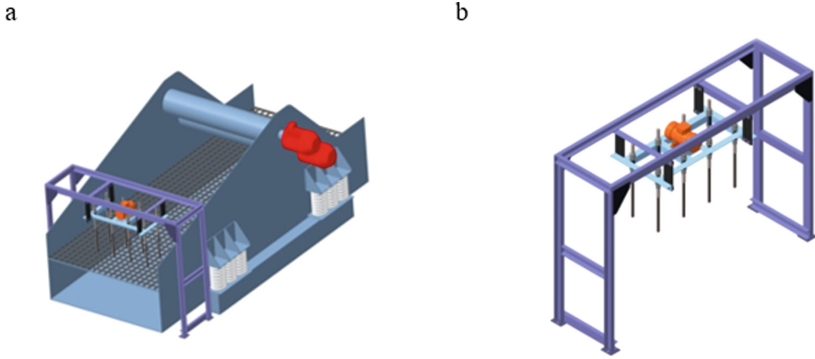


**Fig. 3.** Vibroscreen with feed elements: a - general view of vibrating screen with FE; b - feed elements.

**Table 1.** Data of platform material (Steel 20, GOST 1050-2013).

1	Yield stress (MPa)	235
2	The modulus of normal elasticity (MPa)	200 000
3	Poisson's ratio	0.3
4	Density ( $\text{kg/m}^3$ )	7 800
5	The temperature coefficient of linear expansion ( $1/\text{C}$ )	0.000012
6	Thermal conductivity (W/m C)	55
7	Compressive strength (MPa)	410
8	Tensile strength (MPa)	209
9	Torsional fatigue strength (MPa)	139

**Table 2.** Data of feed elements material (Steel 45, GOST 1050-2013).

1	Yield stress (MPa)	560
2	The modulus of normal elasticity (MPa)	210 000
3	Poisson's ratio	0.3
4	Density ( $\text{kg/m}^3$ )	7 810
5	The temperature coefficient of linear expansion ( $1/\text{C}$ )	0.000013
6	Thermal conductivity (W/m C)	47
7	Compressive strength (MPa)	600
8	Tensile strength (MPa)	294
9	Torsional fatigue strength (MPa)	150

Stress analysis shows their growth for material “B”, which is very clearly seen when comparing the FE in Fig. 6, where the middle of the area working with material “B” acquired tints of stresses corresponding to high numerical values of the color scale (Table 4).

**Table 3.** Parameters and results of feed element location.

	Description	Value
1	Element type	10-nodal tetrahedrons
2	Maximum length of the element side (mm)	10
3	The maximum coefficient of condensation on the surface	5
4	The coefficient of vacuum in the volume	3.5
5	Number of finite elements	114953
6	Number of nodes	235487

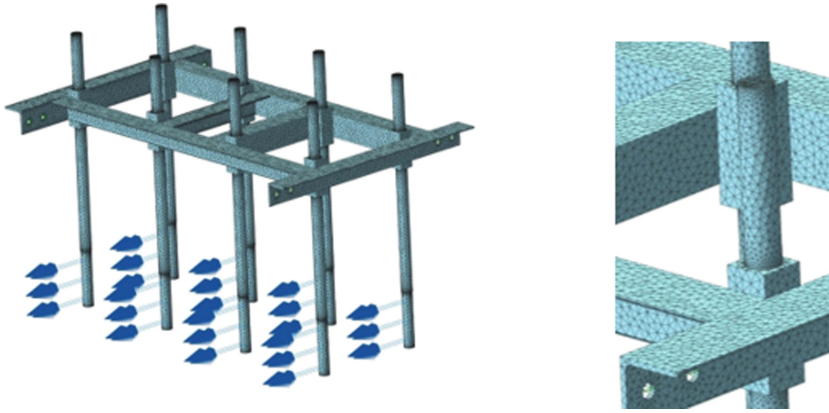


**Fig. 4.** Finite element grid of the FE construction (a) and its fragment enlarged (b), consisting of tetrahedron grid of finite elements.

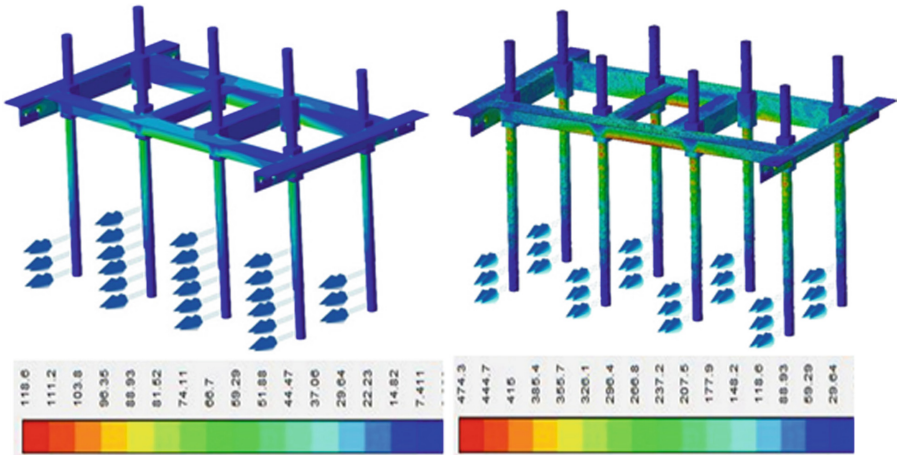


**Fig. 5.** Equivalent Mises stress of feed elements platform for various bulk materials.

Accordingly, the total linear displacement, USUM (mm), also varied from (0) to a maximum of 3.905783 for bulk material “A” and from 0 to 15.623117 for material “B” (Fig. 6).

As a result of the numerical analysis of the researched system, a picture of the safety factor distribution by structural elements was obtained, expressed by the range of its change. The obtained values of the safety factor ranged from 3.457605 to 1000 for bulk material “A” and from 0.8644 to 1000 for material “B” (Fig. 7). As can be seen from the results of the analysis, the loading regime of the structure for material “A” is safe, as indicated by the value of the minimum safety factor of 3.5. And for material “B”, the minimum safety factor is 0.8, which is much less than 3.5. Consequently, the load from the material “A” practically does not affect the efficiency of the FE. The simulated design demonstrated a large safety margin, confirmed by the resulting safety factor.

The scale of the FE image shown in Fig. 7 does not allow us to clearly compare the color variations of the finite element grid, which confirm changes in the calculated values of the coefficient for the loads considered from the action of various materials, but the color gradient decoding below each of the figures shows numerically a significant difference in the indices strength.

Based on the results of modeling and calculation, there were no large deformations or stresses in the structure exceeding the yield strength of the material

**Table 4.** Inertial characteristics of FE models.

	Name	Value
1	Mass of the model (kg)	55.81
2	Center of the model gravity (m)	(0.000011; -0.117649; -0.000087)
3	The inertia moment of the model relative to the mass center (kg m <sup>2</sup> )	(8.229942; 7.831576; 3.248618)
4	The reactive moment with respect to the mass center (N m)	For bulk material “A” (0.656308; -47.820212; -1151.888135) For bulk material “B” (2.639079; -191.280431; -4607.557001)
5	The total reaction of supports (N)	For bulk material “A” (-3057.227214; 0.157531; -1.370206) For bulk material “B” (-12228.908843; 0.630143; -5.480826)
6	The absolute value of the reaction (N)	For bulk material “A” 3057.227525 For bulk material “B” 12228.910087
7	The absolute value of the moment (N m)	For bulk material “A” 1152.880514 For bulk material “B” 4611.526502



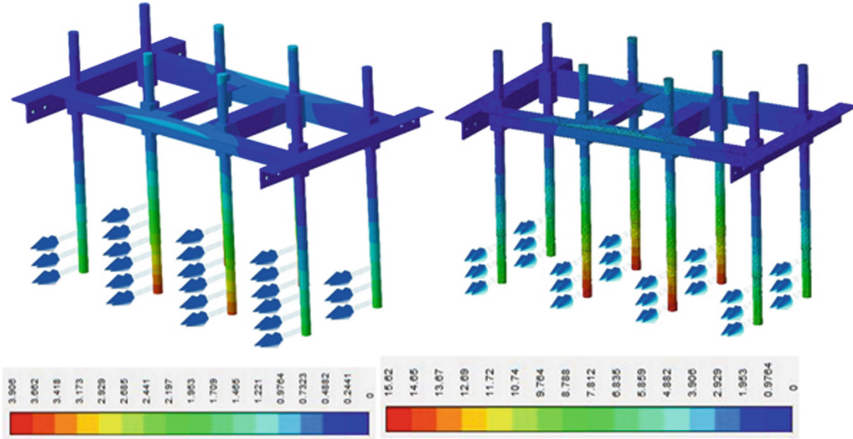


**Fig. 6.** Distribution of the total linear displacement on the platform. (Color figure online)

when the two materials “A” and “B” were screened, so there was no point in re-solving the problem with the new data.

An exception can be given by a material with special properties that increases the force of the pressure on feed elements an order of magnitude because of its increased density or the adhesion coefficient. The above calculations and modeling were made for the average statistical and widely used materials in the construction. The finite element method gave an approximate, nocturnal solution for the physically and geometrically linear rods of feed elements of the screen, greatly simplifying the final system of equations, determining and showing the reliability of the chosen design.

### 3 Experiment

The main test of any calculation results is physical experiment. Considering that the above simulation and calculations represent only feed elements simulation of the real design and how accurate the model and mathematical apparatus implementing this model depend on the experimental verification results. Therefore, on the results of the finite element analysis, a natural, industrially applicable platform with feed elements was installed (Fig. 8). The vibroengine is mounted on the platform with the possibility of changing the amplitude and frequency oscillation, tested for durability and reliability in actual production conditions. A comparison was made between the calculated and actual screen weediness, the dependence of sieve weediness on feed elements number, the sieve weediness dependence on the number of FEs rows, the actual and calculated screen weediness was analyzed, by varying the sieve oscillation frequency.

In the experiment, material 2 moving along the sieve 1, under the influence of vibrations generated by the vibration engine 5, is divided into upper and

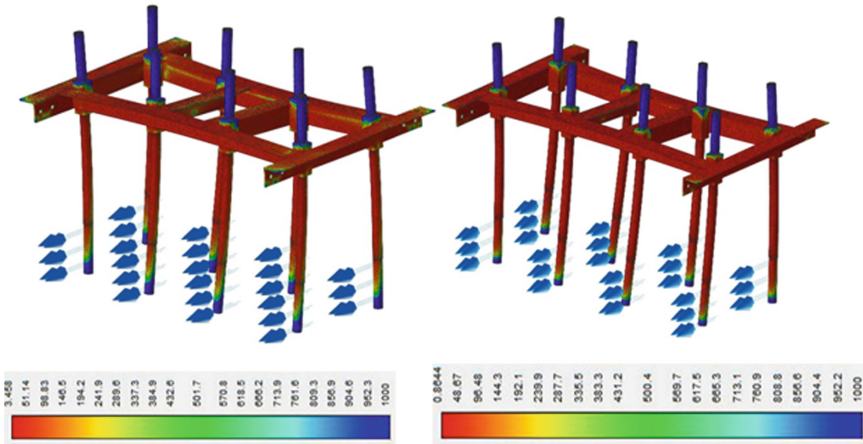


**Fig. 7.** Distribution of the safety factor for strength on the platform. (Color figure online)

lower fractions. The elastic supports 4 provide the mobility of the box with the screen 1 for generating oscillatory movements. The vibroengine works at a constant speed. Particles of bulk material 2 moving along the screen 1 run into feed elements 7 fixed to the frame 6, which leads to the creation of additional chaotic movements of particles in the upper layers of bulk material 2, either coinciding or differing from the direction of the forced oscillations reported by the engine 5.

This increases the difference in the speed of bulk material particles relative to each other, which activates the process of passing particles of lower fraction to the screen surface through the entire layer of bulk material, which increases the screening process efficiency, as a result, increases the screening capacity while maintaining quality sorting.

To determine the efficiency of the FEs operation, it is necessary to identify the most efficient operating mode without FE. For this purpose the following parameters varied: the amplitude of the sieve A oscillation (0.75–3.0 mm) and the vibration frequency  $\nu$  (8–50 Hz).

After revealing the most rational operating mode of the vibration screen without FE, it is necessary to determine the most effective operating mode of the screen with FE, for this purpose the following parameters were changed: the number of FEs in a row from 1 to 10; the number of FEs rows from 1 to 5.

In this case, the EE are installed at a distance of 200 mm from the beginning of the screening and at a height of 10 mm from the screen, these parameters are established in preliminary experimental studies.

The experiment results on determining the influence of the FE number on the screen weed are given in Table 5, and the graph of the sieve weed dependence on the number of FEs is shown (Fig. 9).



**Fig. 8.** Industrial platform with feed elements (1 row), installed in the trough of the vibroscreen on the basis of data analysis of finite element modeling.

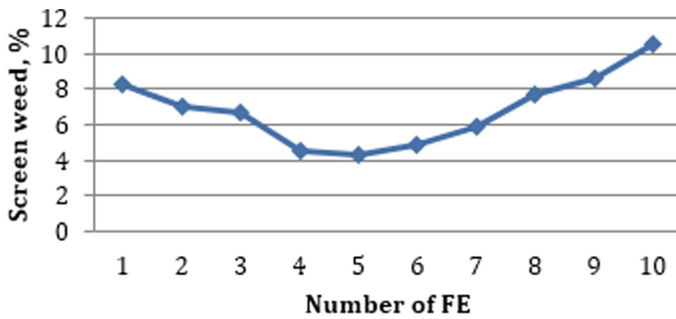


**Fig. 9.** Graph of the sieve weediness dependence on the number of feed elements.

**Table 5.** Test results with different number of FE.

FEs number	Weight, g		Screening time (min)	Weediness of the upper class ZB, %
	Above the sieve	Under the sieve		
1	15 112	6 378	1.40	8.31
2	15 000	6 340	1.38	7.01
3	14 650	6 150	1.40	6.62
4	14 770	6 280	1.36	4.55
5	14 830	6 240	1.36	4.31
6	14 770	6 280	1.36	4.91
7	14 650	6 150	1.34	5.92
8	14 760	6 310	1.34	7.71
9	14 760	6 310	1.33	8.59
10	15 100	6 230	1.32	10.56

**Table 6.** Test results with different number of FEs rows.

FEs number	Weight, g		Screening time (min)	Weediness of the upper class ZB, %
	Above the sieve	Under the sieve		
1	14 830	6 240	1.36	4.31
2	14 530	6 000	1.36	3.5
3	14 550	6 001	1.36	3.51
4	14 530	6 002	1.36	3.52
5	14 489	6 590	1.36	3.79
6	14 552	6 590	1.36	4.52
7	14 466	6 590	1.36	4.78
8	14 588	6 587	1.37	5.59
9	14 003	6 004	1.35	6.98
10	14 554	6 001	1.35	7.99

Further, tests are carried out with a variation of the FE series (Table 6) and an experimental dependence is illustrated (Fig. 10).

On the graph (Fig. 10) the following processes are shown: the lowest index of contamination is reached with the number of rows - from 2 to 10, thus, with the same indices of the minimum level of contamination, a decision is made for further experiments of 2 rows of FE with 5 rods in each row.

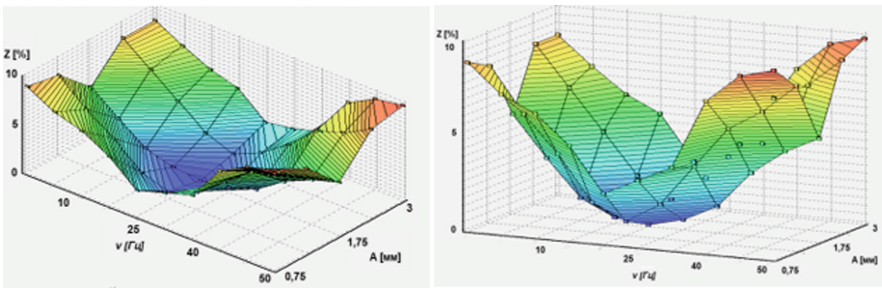


**Fig. 10.** Graph of the screening weed dependence against the frequency of sieve oscillations, the amplitude of sieve vibrations and the number of FEs, under different inclination angles of the coordinate axes.

The evaluation of the strength and rigidity characteristics of the structure (stresses, deformations, displacement of various points in the structure) by finite elemental analysis is fully confirmed in industrial design tests.

To represent the experiment results, multidimensional graph is shown (Fig. 10); the same 3D image of the screening weed, for greater clarity, is shown at different angles of inclination.

The results of experimental studies show a reduction in the level of the upper fraction contamination up to 3.5%, which confirms an increase in the productivity of the screening process, with the same energy consumption, which leads to the conclusion that it is decreasing.

Thus, according to the experimental results, the most effective mode of the vibroscreening process with a 3.5% weed was detected, with an amplitude of sieve vibrations  $A = 2$  mm, a sieve vibrational frequency  $\nu = 25$  Hz, a number of FEs in the FEe series of 5 and the number of FEs rows equal to  $N = 5$ , the time of material passage along the screen was accelerated to  $t = 1.36$  min. Consequently, with a normative screen weed of 5%, the productivity of the screening process increased by 2.1%, and the process time decreased by 4.4%.

Experimental studies confirmed the theoretical premise that the additional material stimulation on the screen, when compared with the standard screening on a flat screen, provides an increase in the productivity of the screening process by 2.1%, a decrease in the material passage time through the screen by 4.4%, while maintaining normative weed of the material is 5%.

The practical significance of the work is confirmed by the using of prototypes of the vibrating screen with additional feed elements in LLP "CS RNP" in Ust-Kamenogorsk in 2017.

## 4 Conclusion

1. The simulation model with the finite element method, in contrast to full-scale manufacturing, allows determining the weak places in the design at the design stage and approaching the task of optimal parameters selection. The finite element analysis of the feed elements platform is the best and accurate method of researching and predicting the operability of the structure under given operating conditions, allowing selecting the parameters of the future design reasonably prior to its industrial manufacture.
2. The application of the mathematical apparatus (FEM) simplifies the construction of an object model consisting of a finite elements set. FEM allows obtaining a solution in the form of stress and strain fields in practically any section of the element. These advantages of the method have not yet been used in the design of vibroscreen elements. Their implementation can reduce the metal equipment consumption, increase the reliability of its operation and reduce self-cost and, ultimately, improve the quality of the sorted material.
3. Computer simulation technology with the help of FEM allows reliable determination of the real operational characteristics of products, helps customers to ensure that their products comply with the necessary requirements and standards.
4. The results of experimental studies of FEs, produced according to the results of the FEM analysis, showed a decrease in the level of sieve weed up to 3.5%, which allows increasing the productivity of the screening process and also reducing the energy consumption.

5. Experimental studies confirmed the theoretical premise that the additional material stimulation on the screen, when compared with the standard screening on a flat screen, provides an increase in the productivity of the screening process by 2.1%, a decrease in the material passage time through the screen by 4.4%, while maintaining normative weed of the material is 5%.

## References

1. Kim, A., Doudkin, M., Vavilov, A., Guryanov, G.: New vibroscreen with additional feed elements. *Arch. Civ. Mech. Eng.* **17**(4), 786–794 (2017). <https://doi.org/10.1016/j.acme.2017.02.009>
2. Stryczek, J., Banas, M., Krawczyk, J., Marciniak, L., Stryczek, P.: The fluid power elements and systems made of plastics. *Procedia Engineering* **176**, 600–609 (2017). [www.elsevier.com/locate/procedia](http://www.elsevier.com/locate/procedia)
3. Doudkin, M., Pichugin, S., Fadeev, S.: Contact force calculation of the machine operational point. *Life Sci. J.* **10**(39), 246–250 (2013). <http://www.lifesciencesite.com>
4. Doudkin, M., Vavilov, A., Pichugin, S., Fadeev, S.: Calculation of the interaction of working body of road machine with the surface. *Life Sci. J.* **133**, 832–837 (2013). <http://www.lifesciencesite.com>
5. Giel, R., Mlyńczak, M., Plewa, M.: Evaluation method of the waste processing system operation. In: *Risk, Reliability and Safety: Innovating Theory and Practice - Proceedings of the 26th European Safety and Reliability Conference, ESREL (2016)*
6. Fedotov, A.I., Młyńczak, M.: Simulation and experimental analysis of quality control of vehicle brake systems using flat plate tester. In: Zamojski, W., Mazurkiewicz, J., Sugier, J., Walkowiak, T., Kacprzyk, J. (eds.) *Dependability Engineering and Complex Systems. AISC*, vol. 470, pp. 135–146. Springer, Cham (2016). [https://doi.org/10.1007/978-3-319-39639-2\\_12](https://doi.org/10.1007/978-3-319-39639-2_12)
7. Bojko, A., Fedotov, A.I., Khalezov, W.P., Mlyńczak, M.: Analysis of brake testing methods in vehicle safety. In: *Safety and Reliability: Methodology and Applications - Proceedings of the European Safety and Reliability Conference, ESREL (2014)*
8. Surashev, N., Dudkin, M., Yelemes, D., Kalieva, A.: The planetary vibroexciter with elliptic inner race. *Advanced Materials Research*, vol. 694–697, pp 229–232. Trans Publications, Switzerland (2013). <https://doi.org/10.4028/www.scientific.net/AMR.694-697.229>
9. Doudkin, M.V., Fadeyev, S.N., Pichugin, S.Y.: Studying the machines for road maintenance. *Life Sci. J.* **10**(12), 134–138 (2013). (ISSN1097–8135). <http://www.lifesciencesite.com>
10. Doudkin, M.V., Pichugin, S.Y.U., Fadeyev, S.N.: The analysis of road machine working elements parameters. *World Appl. Sci. J.* **23**(2), 151–158 (2013). (ISSN/E-ISSN: 1818–4952/1991-6426). IDOSI Publications. <https://doi.org/10.5829/idosi.wasj.2013.23.02.13061>
11. Doudkin, M., Kim, A., Kim, V.: Application of finite elements method for modeling and analysis of feed elements stresses of the vibroscreen. In: *Proceedings of the 14th International Scientific Conference: Computer Aided Engineering, Politechnika Wroclawska*, 8 p. (2018)
12. Kapaeva, S., Bergander, M., Vakhguelt, A., Khairaliyev, S.: Ultrasonic evaluation of the combined effect of corrosion and overheating in grade 20 steel water-wall boiler tubes. *INSIGHT* **59**(12), 637–643 (2017). ISSN 1354–2575

13. Azamatov, B.N., Ozhikenov, K.A., Azamatova, Z.K.: Assessment of the effectiveness of the use of palladium in catalytic SHS-units for diesel engines. *News Natl. Acad. Sci. Repub. Kazakhstan, Ser. Geol. Tech. Sci.* **4**(424), 142–147 (2017)
14. Ozhikenov, K.A., Mikhailov, P.G., Ismagulova, R.S., Azamatova, Z.K., Azamatov, B.N.: Development of technologies, methods and devices of the functional diagnostics of microelectronic sensors parts and components. In: 2016 13th International Scientific-Technical Conference on Actual Problems of Electronic Instrument Engineering, APEIE 2016 - Proceedings, vol. 1, pp. 84–90 (2016). <https://doi.org/10.1109/APEIE.2016.7802218>
15. Azamatov, B.N., Kvassov, A.I., Azamatova, Z.K.: Hydrocyclones set ACS with variable geometry in the HAR TPP system. In: 2017 International Conference on Industrial Engineering, Applications and Manufacturing, ICIEAM 2017 - Proceedings (2017). <https://doi.org/10.1109/ICIEAM.2017.8076132>
16. Kapaeva, S., Bergander, M., Vakhguelt, A., Khairaliyev, S.: Remaining life assessment for boiler tubes affected by combined effect of wall thinning and overheating. *J. Vibroengineering JVE* **19**(8), 5892–5907 (2017)
17. Kapaeva, S., Bergander, M., Vakhguelt, A.: Combination non-destructive test (NDT) method for early damage detection and condition assessment of boiler tubes. *Procedia Eng.* **188**, 125–132 (2017). ISSN 1877–7058